THE JOURNAL OF BIOLOGICAL CHEMISTRY VOL. 287, NO. 3, pp. 2119–2129, January 13, 2012

Structural and Kinetic Evidence That Catalytic Reaction of Human UDP-glucose 6-Dehydrogenase Involves Covalent Thiohemiacetal and Thioester Enzyme Intermediates*[S]

Received for publication, October 12, 2011, and in revised form, November 24, 2011 Published, JBC Papers in Press, November 28, 2011, DOI 10.1074/jbc.M111.313015

Sigrid Egger[‡§], Apirat Chaikuad[¶], Mario Klimacek[‡], Kathryn L. Kavanagh[¶], Udo Oppermann[¶‖], and Bernd Nidetzky[‡§1]

From the [‡]Institute of Biotechnology and Biochemical Engineering, Graz University of Technology, A-8010 Graz, Austria, [¶]Structural Genomics Consortium, University of Oxford, Old Road Campus Research Building, Oxford OX3 7DQ, United Kingdom, [‖]Botnar Research Centre, National Institute for Health Research Oxford Biomedical Research Unit, University of Oxford, Oxford OX3 7LD, United Kingdom, and [§]Austrian Centre of Industrial Biotechnology, A-8010 Graz, Austria

Background: Human UDP-glucose 6-dehydrogenase (hUGDH) is responsible for biosynthesis of UDP-glucuronic acid.
Results: We report the crystal structure of a thiohemiacetal enzyme intermediate and demonstrate kinetic trapping of a thioester enzyme intermediate.
Conclusion: Covalent catalysis by Cys^{276} is established. Glu^{161} functions as a Brønsted base for hydrolysis of the thioester enzyme intermediate.
Significance: A detailed mechanism for covalent catalysis by hUGDH is proposed.

Biosynthesis of UDP-glucuronic acid by UDP-glucose 6-dehydrogenase (UGDH) occurs through the four-electron oxidation of the UDP-glucose C6 primary alcohol in two NAD^+-dependent steps. The catalytic reaction of UGDH is thought to involve a Cys nucleophile that promotes formation of a thiohemiacetal enzyme intermediate in the course of the first oxidation step. The thiohemiacetal undergoes further oxidation into a thioester, and hydrolysis of the thioester completes the catalytic cycle. Herein we present crystallographic and kinetic evidence for the human form of UGDH that clarifies participation of covalent catalysis in the enzymatic mechanism. Substitution of the putative catalytic base for water attack on the thioester (Glu^{161}) by an incompetent analog (Gln^{161}) gave a UGDH variant (E161Q) in which the hydrolysis step had become completely rate-limiting so that a thioester enzyme intermediate accumulated at steady state. By crystallizing E161Q in the presence of 5 mM UDP-glucose and 2 mM NAD^+, we succeeded in trapping a thiohemiacetal enzyme intermediate and determined its structure at 2.3 Å resolution. Cys^{276} was covalently modified in the structure, establishing its role as catalytic nucleophile of the reaction. The thiohemiacetal reactive C6 was in a position suitable to become further oxidized by hydride transfer to NAD^+. The proposed catalytic mechanism of human UGDH involves Lys^{220} as general base for UDP-glucose alcohol oxidation and for oxyanion stabilization during formation and breakdown of the thiohemiacetal and thioester enzyme intermediates. Water coordinated to Asp^{280} deprotonates Cys^{276} to function as an aldehyde trap and also provides oxyanion stabilization. Glu^{161} is the Brønsted base catalytically promoting the thioester hydrolysis.

UDP-glucose 6-dehydrogenase (UGDH; EC 1.1.1.22)[2] catalyzes the conversion of UDP-glucose (UDP-Glc) to UDP-glucuronic acid (UDP-GlcUA). The enzyme is responsible for biosynthesis of UDP-GlcUA in a multitude of species, including humans (1). UGDH fuels various cellular metabolic pathways including the production of extracellular matrix glycosaminoglycans such as hyaluronan, the synthesis of rare sugars, and detoxification metabolism (2). Crystal structures of the human and bacterial forms of UGDH have illustrated the basic anatomy of the enzyme (3–7). UGDH folds into oligomers with each protein subunit composed of two α/β domains that are connected by a large central α-helix. The N-terminal domain is responsible for binding of NAD^+, UDP-Glc is bound by interactions from both domains, and the active site is located in the interdomain cleft. Sequence analysis has shown that elementary features of UGDH structure and function have been conserved across the three superkingdoms of life (1). Active-site residues are essentially invariant among members of the UGDH enzyme family (1). The homodimeric quarternary structure adopted by bacterial UGDHs such as that from *Streptococcus pyogenes* (*Sp*UGDH) (3) appears to be the basic structural unit

* This work was supported by the Austrian Science Fund (DK Molecular Enzymology W901-B05) and the Structural Genomics Consortium registered charity (no. 1097737) funded by the Wellcome Trust, GlaxoSmithKline, Genome Canada, the Canadian Institutes of Health Research, the Ontario Innovation Trust, the Ontario Research and Development Challenge Fund, the Canadian Foundation for Innovation, Vinnova, the Swedish Strategic Research Foundation, the Knut and Alice Wallenberg Foundation, and the Karolinska Institute. This work was also further supported by the National Institute for Health Research Oxford Biomedical Research Unit.
⌘ *Author's Choice*—Final version full access.
[S] This article contains supplemental procedures, Table S1, Figs. S1–S5, and Scheme S1.
[1] To whom correspondence should be addressed: Institute of Biotechnology and Biochemical Engineering, Graz University of Technology, Petersgasse 12/1, A-8010 Graz, Austria. Tel.: 43-316-873-8400; Fax: 43-316-873-8434; E-mail: bernd.nidetzky@tugraz.at.

[2] The abbreviations used are: UGDH, UDP-Glc 6-dehydrogenase; hUGDH, UGDH from *Homo sapiens*; UDP-Glc, UDP-α-D-glucose; UDP-GlcUA, UDP-α-D-glucuronic acid; *Sp*UGDH, UGDH from *S. pyogenes*; PDB, Protein Data Bank; GAPN, glyceraldehyde 3-phosphate dehydrogenase.

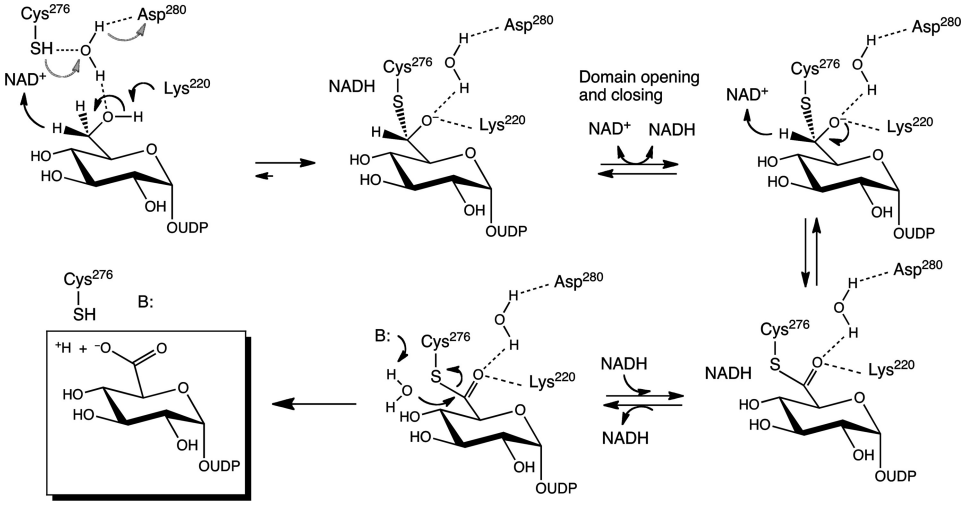

SCHEME 1. **Proposed catalytic mechanism of UGDH, based on the evidence from prior studies of UGDH orthologs from *S. pyogenes*, bovine liver, and man.**

of UGDH enzyme function. The human UGDH enzyme (hUGDH) is arranged into a disc-shaped trimer of such dimers (4, 5). The more complex oligomeric architecture of hUGDH as compared with *Sp*UGDH is typical for UGDH from eukaryotic origin (1, 4, 5) but otherwise does not involve a recognizable gain of enzymatic function.

Chemically, the reaction of UGDH is a four-electron oxidation of the C6 alcohol group of UDP-Glc, occurring in two NAD^+-dependent steps (Equation 1).

$$\text{UDP-Glc} + 2\,\text{NAD}^+ + \text{H}_2\text{O} \rightarrow \text{UDP-GlcUA} + 2\,\text{NADH} + 2\,\text{H}^+ \quad \text{(Eq. 1)}$$

After early elegant studies of the UGDH mechanism performed with bovine liver enzyme (8–16), work of Tanner and co-workers (3, 17–20) with *Sp*UGDH has led to the current proposal for the catalytic mechanism (Scheme 1). In this mechanism the active-site Cys has the role of a catalytic nucleophile that intercepts the C6 aldehyde produced in the first step of substrate oxidation, resulting in formation of a covalent thiohemiacetal enzyme intermediate. After replacement of NADH by NAD^+, the reaction proceeds by converting the thiohemiacetal into a thioester. Hydrolysis of the thioester enzyme intermediate yields the UDP-GlcUA product.

Recent studies of hUGDH (4, 21, 22) have advanced knowledge of the mechanism (Scheme 1), showing that binding of NAD^+ to an initially formed complex of enzyme and UDP-Glc is accompanied by a large rigid-body movement of the N-terminal domain, resulting in seclusion of substrate and coenzyme in their reactive positions through interdomain closure. Coenzyme exchange at the stage of thiohemiacetal enzyme intermediate, therefore, necessitates a full cycle of domain opening (release of NADH) and closing (binding of NAD^+), and this overall step was shown to be rate-determining for the human enzyme reaction in the presence of physiological concentrations of NAD^+.

Useful evidence in support of covalent catalysis by UGDH was obtained from the characterization of site-directed mutants in which the candidate nucleophile (*Sp*UGDH:Cys^{260}; hUGDH:Cys^{276}) had been replaced by a serine (4, 17). The Cys-to-Ser mutants were almost inactive under standard assay conditions. However, their incubation in the presence of NAD^+ and UDP-Glc led to accumulation of a stable enzyme adduct that was shown by mass spectrometry (MS) to be derived from covalent attachment of the oxidized substrate. It was further demonstrated for *Sp*UGDH (17) that the introduced Ser^{260} had become acylated with UDP-GlcUA. Hydrolysis of the unnatural ester linkage in the C260S mutant was thought to proceed at a very slow rate, thus allowing accumulation of the intermediate. Crystal structures of an unreactive ternary complex of wild-type *Sp*UGDH (UDP-xylose/NAD^+) and the C260S mutant (UDP-GlcUA/NADH) showed that Cys^{260} and Ser^{260} were both brought into positions suitable for participation in covalent catalysis (3). In hUGDH ternary complex structures (UDP-Glc/NADH; UDP-GlcUA/NAD^+), Cys^{276} was likewise placed appropriately to function as a catalytic nucleophile (4). Nonetheless, the proposed covalent intermediates (enzyme bound thiohemiacetal and thioester species) in the catalytic mechanism of UGDH (Scheme 1) are subject to the caveat of missing direct affirmation for their formation in the course of the enzymatic reaction. Observation of acylenzyme development on Ser^{260} in the *Sp*UGDH mutant (17) may not be directly applicable to the situation of the wild-type enzyme where the native Cys^{260} offers a substantially different chemical reactivity as nucleophile or otherwise.

A C260A mutant of *Sp*UGDH readily oxidized the chemically synthesized aldehyde (UDP-*gluco*-hexodialdose; hydrated form) to UDP-GlcUA, whereas the same enzyme was inactive when offered UDP-Glc as substrate. The analogous C276A mutant of hUGDH was capable of catalyzing the oxidation of UDP-Glc to UDP-GlcUA, however, at a very low rate (4). Collectively, these findings could be interpreted to mean that the second oxidation step of the UGDH reaction might occur even in the absence of a catalytic nucleophile. In contrast, Ridley *et al.* (11) showed that a cyanide-derivatized form of bovine liver UGDH was even more active than the unmodified enzyme in reduction of UDP-*gluco*-hexodialdose, whereas only the

unmodified enzyme was reactive in the oxidation of the same substrate. It becomes apparent, therefore, that covalent catalysis by cysteine is not fundamentally well understood in its molecular basis, and despite the significant research efforts in different groups, the catalytic mechanism of UGDH remains elusive.

We wish to communicate herein a study of hUGDH that provides clarification. Using site-directed replacement of the presumed catalytic base for hydrolysis of thioester (Glu^{161}) by an incompetent analog (Gln), we found that the rate of the hydrolysis step had become selectively reduced in the E161Q mutant, thus allowing buildup of a thioester enzyme intermediate at steady state. By crystallizing the E161Q mutant under conditions of a limiting concentration of NAD^+ while UDP-glucose was present in saturating amounts, we succeeded in intercepting a thiohemiacetal enzyme intermediate in the crystal and determined its structure at 2.3 Å resolution. With this structure the mechanism of covalent catalysis by Cys^{276} can be settled. However, the structure of the E161Q intermediate has two additional aspects of relevance. First, it shows that the protein subunit adopts an apoenzyme-like "open domain" conformation and does not contain a NAD(H) ligand at the coenzyme binding site, indicating that the mutant has actually undergone intermittent domain opening to allow for the release of NADH from the thiohemiacetal enzyme intermediate, as proposed recently (4). Second, there is appreciable interest in the development of antagonists of hUGDH (23, 24). The relevant form of the enzyme to be targeted with reversible inhibitors is the thiohemiacetal intermediate, which accumulates at the steady state (4). By studying mutants of two other prominent residues in the active site of hUGDH (Lys^{220} and Asp^{280}; Refs. 1, 21, and 22), we have also delineated the steps in catalysis that lead up to the thiohemiacetal intermediate. Finally, comparison of wild-type enzyme and E161Q in pH studies gave clear evidence in support of a general base catalytic function of Glu^{161} in the hydrolysis step of the reaction. For the first time, therefore, a comprehensive catalytic mechanism for hUGDH is proposed.

EXPERIMENTAL PROCEDURES

Materials—Unless stated otherwise, all materials were of the highest purity available from Sigma. NAD^+ was obtained from Roth (Karlsruhe, Germany) in a purity of >98%.

Site-directed Mutagenesis and Preparation of Enzymes—The enzyme referred to as native or wild-type hUGDH is a truncated version of the natural enzyme that lacks 27 amino acids from the C terminus. It was previously shown that the truncation neither affects the enzyme activity nor the homohexameric oligomerization of hUGDH in solution (4). Variants of hUGDH likewise contain the C-terminal truncation. Mutagenesis leading to site-directed substitution of Glu^{161} by Gln (E161Q), Lys^{220} by Ala (K220A), Asp^{280} by Ala (D280A), Thr^{131} by Ser (T131S), and Asn^{224} by Ala (N224A) was performed employing the Stratagene QuikChange site-directed mutagenesis kit according to standard protocols and using the wild-type gene as template. The oligonucleotide primers used are listed in the supplemental procedures. The mutants were recombinantly produced in *Escherichia coli* BL21(DE3)-R3 using a pBEN-derived plasmid vector, encoding the target protein fused to an N-terminal extension that harbors a solubility enhancement tag, a streptavidin tag, and a tobacco etch virus protease cleavage site. Enzymes were purified using a previously described three-step procedure consisting of affinity chromatography, gel filtration (Superdex 200 16/60 HiLoad, GE Healthcare), and anion exchange chromatography (HiTrap-Q HP, GE Healthcare) (4). The N-terminal extension was removed before gel filtration using tobacco etch virus protease. Details of the procedures are given elsewhere (4). All mutants were shown by gel filtration analysis to form hexamers in solution, as does native hUGDH.

TABLE 1
Crystallographic data collection and refinement statistics

	E161Q mutant (thiohemiacetal intermediate)
Data collection	
PDB accession code	3khu
Synchrotron beamline	Diamond I03
Wavelength (Å)	0.9763
Space group	$P2_12_12$
Unit cell dimensions	$a = 203.5$, $b = 207.3$, $c = 93.4$ Å $\alpha = \beta = \gamma = 90.0°$
Resolution range[a] (Å)	48.74–2.30 (2.42–2.30)
No. unique reflections[a]	175,128 (25,412)
Completeness[a] (%)	99.8 (100.0)
$\langle I/\sigma(I)\rangle$[a]	9.4 (2.0)
R_{merge}[a]	0.106 (0.743)
Redundancy[a]	4.3 (4.3)
Refinement	
No. Atoms P/L/O[b]	21,866/432/1397
R_{work}/R_{free}	0.195/0.225
r.m.s.d. bond length[c] (Å)	0.016
r.m.s.d. bond angle[c] (°)	1.438
B_{mean} P/L/O[b] (Å^2)	23.9/42.9/27.5

[a] Values in parentheses show the statistics for the highest resolution shells.
[b] P/L/O represents protein/ligand/other (water, ion, and solvent).
[c] r.m.s.d. indicates root mean square deviation.

Crystallization of E161Q, Data Collection, and Refinement—The E161Q protein solution containing 2 mM NAD^+ and 5 mM UDP-Glc was concentrated to 15 mg/ml (~0.3 mM). Crystals were grown at 4 °C in 150-nl sitting drops, equilibrated against mother liquor containing 18% PEG "smears" (a mixture of ten PEG polymers with molecular masses ranging from 400 to 10000 Da), 5% ethylene glycol, and 0.1 M HEPES (pH 7.5). Diffraction data were collected at 100 K at Diamond beamline I03. Data were processed with MOSFLM (25, 26) and subsequently scaled using the program SCALA (25). The structure of E161Q was solved by molecular replacement using the Phaser (27) program and the structure of hUGDH (PDB code 2q3e) as the search model. The structure was manually rebuilt in COOT (28), and restrained refinement with appropriate TLS groups was performed using REFMAC5 (29). Data collection and refinement statistics are summarized in Table 1.

Enzyme Kinetics—Reactions were performed at 25 (± 1) °C in potassium phosphate buffer (50 mM; pH 7.5). Initial rates were obtained by measuring the absorbance of NADH produced at 340 nm ($\epsilon_{NADH} = 6220\ M^{-1}\ cm^{-1}$). The duration of the reaction was between 10 and 350 min, depending on the activity of the enzyme used. Unless mentioned otherwise, initial rates were obtained under conditions in which the applied enzyme had undergone at least three turnovers. Measurements were performed in triplicate, and the data were averaged. Kinetic parameters (V_{max}, K_m) were calculated from initial-rate data

recorded at varied concentrations of UDP-Glc or NAD^+ using a constant saturating concentration of the respective other substrate (15 mM NAD^+, 4 mM UDP-Glc). Turnover numbers (k_{cat}) were calculated by dividing $\frac{1}{2}V_{max}$ (2 NADH produced/1 UDP-Glc converted) with the molar concentration of enzyme active sites (E). The protein concentration was determined from the absorbance at 280 nm using a molar extinction coefficient of 48360 $M^{-1}cm^{-1}$ (30). K_{mS} is the K_m for UDP-Glc substrate, and K_{mC} is the K_m for NAD^+ coenzyme.

The E161Q mutant was characterized in stopped-flow kinetic experiments performed according to procedures described elsewhere (4). Reaction time courses were recorded in triplicate and averaged. The limiting concentration of enzyme active sites was in the range 10–15 μM. A solution of E161Q saturated with UDP-Glc (1 mM) was mixed with a solution containing UDP-Glc (1 mM) and NAD^+ (0.2–20 mM). Suitable controls were obtained by mixing reaction solutions lacking the enzyme. Apparent first-order rate constants (k_{obs}) for the kinetic transient were obtained from an appropriate fit of the stopped-flow progress curves, as described under "Data Analysis" below.

Functional complementation of K220A by externally added primary amines was examined by comparing initial rates measured in the absence and presence of the amine whose concentration was varied in the range 10–500 mM. Experiments were performed at pH values from 6.5 to 9.0. A similar analysis was carried out with D280A studying the effect of external anions on the activity of the mutant (pH 7.5). Chloride, bromide, azide, formate, and acetate were tested as their sodium salts in a concentration range between 10 and 300 mM.

pH Studies—The pH dependences of steady-state kinetic parameters k_{cat} and k_{cat}/K_{mC} were determined in the pH range 5.0–10.5 for wild-type hUGDH. A three-component buffer, composed of MES, Tris, and glycine, was used that displayed a pH-independent ionic strength of 0.1 M. The pH dependence of the apparent k_{cat} for E161Q was determined in the pH range 6.0–9.0. The apparent k_{cat} was obtained from an initial-rate measurement at saturating concentrations of UDP-Glc (5 mM) and NAD^+ (15 mM). The pH dependence of k_{obs} for the wild-type enzyme was obtained in the pH range 6.0–8.5. The concentration of UDP-Glc was 1.0 mM and at each pH k_{obs} was determined at two concentrations of NAD^+ that were either limiting (0.1 mM; $<K_{mC}$) or saturating at the steady state (10 mM).

Data Analysis—Sigma Plot 2004 software (Version 9.01) was used for nonlinear least squares regression analysis. Equation 2 describes NADH formation in multiple turnover stopped flow experiments. $[NADH]_t$ is the concentration of NADH at time t, Π is the [NADH] amplitude of the kinetic transient, V_{ss} is the steady-state rate, and Y_0 stands for the (absorbance) background of the control. Reactions start at Y_0. Equation 3 describes a pH dependence where activity ($Y = k_{cat}$, k_{cat}/K_{mC}, k_{obs}) is constant at high pH and decreases below apparent pK. C is the pH-independent value of Y at the optimum state of protonation. Equation 4 describes a sigmoidal pH dependence with constant values of Y at high (C_H) and low pH (C_L), and an inflection point at pK.

TABLE 2
Kinetic parameters for the E161Q mutant, determined at 25 °C and pH 7.5, in comparison to wild-type hUGDH

	Wild type[a]	E161Q
k_{cat} (s^{-1})	0.85 ± 0.1	0.0014 ± 0.0001
K_{mC} (mM)	0.7 ± 0.1	0.10 ± 0.01
K_{mS} (μM)	35 ± 5	55 ± 10
k_{cat}/K_{mC} ($s^{-1}mM^{-1}$)	1.2	0.014
k_{cat}/K_{mS} ($s^{-1}mM^{-1}$)	24	0.025
k_{obs} (s^{-1})[b]	~10	0.33 ± 0.01
K_{dC} (mM)[c]	0.4	0.16 ± 0.02
$\Pi/[E]$ [−][b]	0.3	1.0 ± 0.1
k_{obs}/K_{dC} ($s^{-1}mM^{-1}$)	25	2.1

[a] Data are from Egger *et al.* (4).
[b] UDP-Glc (1 mM) and NAD^+ (15 mM) were present at saturating concentrations.
[c] Value was obtained from non-linear fits of k_{obs} *vs.* $[NAD^+]$ data with a single rectangular hyperbola function.

$$[NADH]_t = \Pi(1 - e^{-k_{obs}t}) + V_{ss}t + Y_0 \quad \text{(Eq. 2)}$$

$$\log Y = \log [C/(1 + [H^+]/K)] \quad \text{(Eq. 3)}$$

$$\log Y = \log [(C_H + C_L([H^+]/K)/(1 + [H^+]/K))] \quad \text{(Eq. 4)}$$

Mass Spectrometry Analysis—The electrospray ionization-TOF-MS method applied to identify covalent adduct formation in E161Q was described in a previous publication (4).

RESULTS AND DISCUSSION

Kinetic Characterization of E161Q Mutant—Crystal structures of hUGDH in the apo form (PDB code 3itk) and in a ternary complex with UDP-Glc and NADH (PDB code 2q3e) have shown that to bring the nicotinamide ring of NAD^+ into hydride transfer position Glu^{161} must move away from its original place in the active site of the apoenzyme (4). In the reactive conformation of the enzyme, which we believe is represented by the structure of the hUGDH·UDP-Glc/NADH complex, Glu^{161} is drawn away from the nicotinamide by contact with Lys^{129}. A third structure of hUGH in complex with the UDP-GlcUA product and NAD^+ (PDB code 2qg4) revealed that Glu^{161} was conformationally flexible. In half of the enzyme subunits the side chain of Glu^{161} adopted the position inside the active site, resulting in a displacement of the nicotinamide portion of the coenzyme. In the remainder of the subunits, Glu^{161} was in the alternative "out" conformation, and an ordered nicotinamide moiety was observed. This conformational flexibility of Glu^{161} distinguished the product structure from the structure of the substrate complex, where Glu^{161} was found exclusively in the out conformation. Based on this structural evidence, we speculated that Glu^{161} could serve the role of a general base in the catalytic mechanism, assisting the attack of water on the putative thioester intermediate. Therefore, Glu^{161} was a very interesting target for site-directed mutagenesis, and it was replaced by Gln with the aim of disrupting the proposed hydrolysis step.

The purified E161Q mutant displayed a 610-fold decrease in k_{cat} as compared with wild-type hUGDH (Table 2 summarizes results from steady-state and presteady-state kinetics). The catalytic efficiencies for UDP-Glc (k_{cat}/K_{mS}) and NAD^+ (k_{cat}/K_{mC}) were also strongly affected by the mutation. These results indicate that Glu^{161} has an important role for the enzymatic function of hUGDH, and its substitution by Gln affects the catalytic reaction at different steps. The proposed kinetic mecha-

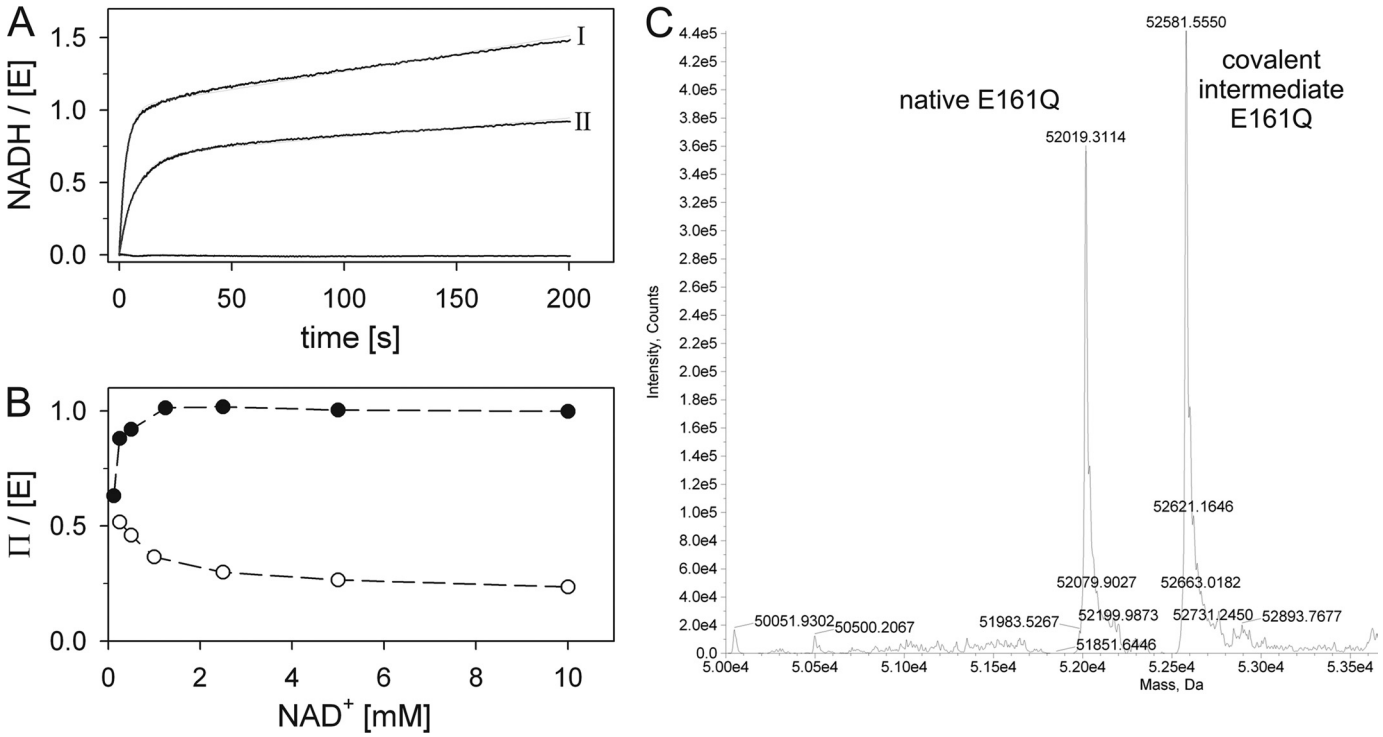

FIGURE 1. **Kinetic and mass spectrometric evidence for stable intermediate accumulation in E161Q.** *A*, shown are typical stopped-flow progress curves of the enzymatic reaction obtained at 10 mM (*I*) or (125 μM (*II*) NAD^+ and 1 mM UDP-Glc using 15 μM enzyme subunits. The *gray lines* are the fit of Equation 1 to the data. A respective reference measurement lacking the enzyme is also shown. *B*, shown is dependence of burst magnitude on the concentration of NAD^+ used in the reaction for E161Q (*filled circles*) and wild-type enzyme (*open circles*; data are from Ref. 4). *C*, shown are deconvoluted data from ESI-MS characterization of a protein sample obtained after a 1-min reaction time from a conversion experiment, performed using 20 μM E161Q, 15 mM NAD^+, and 1 mM UDP-Glc. The *left peak* corresponds to the underivatized mutant protein. The *right peak* shows a mass increase of 562 g/mol, consistent with formation of a thioester enzyme intermediate.

nism of hUGDH (supplemental Scheme S1) implies that k_{cat}/K_{mS} is a direct measure of UDP-Glc binding to the free enzyme (k_1), whereas k_{cat}/K_{mC} is a complex parameter that includes all steps from binding of NAD^+ to enzyme·UDP-Glc (k_3) up to dissociation of NADH from the thioester intermediate (k_9). The k_{cat} involves all unimolecular steps of the mechanism (k_5, k_9, k_{11}, k_{13}). Stopped-flow experiments were, therefore, performed with E161Q to resolve kinetic complexity of the steady-state parameters and to analyze the different parts of the enzymatic reaction (Scheme 1) as kinetically separate steps. The time course of UDP-Glc conversion by E161Q showed a large transient "burst" of NADH formation that was followed by the much slower steady-state phase (Fig. 1*A*). A fit of the data with Equation 2 provided estimates for k_{obs} and the burst amplitude, Π. Reactions were performed at different concentrations of NAD^+, and we show in Fig. 1*B* that the molar ratio of Π and [*E*] (concentration of enzyme subunits used in the reaction) increased with increased NAD^+ concentration and that it approached a value of 1 at high coenzyme levels. This result implies that there is a slow step in the enzymatic reaction of the E161Q mutant that occurs after the formation of NADH, whether the NADH was derived from both oxidation steps in the case that hydrolysis was rate-limiting or only from the first step of alcohol oxidation in the case that aldehyde oxidation was rate-limiting. The contribution of this slow step to overall rate limitation strongly increases when the NAD^+ concentration is raised, as evident from Fig. 1*B*. The catalytic step of thioester hydrolysis lacks NAD^+ dependence, so it is therefore reasonable to assume that the NAD^+-dependent oxidation steps of the reaction, not the hydrolysis step, become accelerated in response to increasing levels of NAD^+. Consequently, the breakdown of the thioester intermediate is strongly suggested to be rate-determining for the E161Q reaction at steady state. Of note, the wild-type enzyme shows a dependence of Π/[*E*] on NAD^+ concentration that is completely opposite that of the E161Q mutant (Fig. 1*B*), with a marked decline of Π/[*E*] at high NAD^+, suggesting overall rate limitation at the step of aldehyde oxidation.

The value of k_{obs} associated with the kinetic transient for the reaction of E161Q at saturating concentration of NAD^+ was 0.33 s^{-1}, which is just 30-fold decreased as compared with the corresponding value of k_{obs} for the wild-type enzyme (10 s^{-1}; Table 2). Therefore, this shows that the disruptive effect of the $Glu^{161} \rightarrow Gln$ mutation was ~20 times stronger on the steady-state constant (k_{cat}) than it was on the transient rate constant (k_{obs}). From the hyperbolic dependence of k_{obs} on NAD^+, we determined an apparent dissociation constant of NAD^+ from enzyme·UDP-Glc (K_{dC}) and show in Table 2 that the ratio k_{obs}/K_{dC} was just 12-fold decreased in E161Q as compared with the wild-type enzyme. In wild-type hUGDH, k_{obs}/K_{dC} stands for the first oxidation step of the reaction (supplemental Scheme S1). The implication of these findings that substitution of Glu^{161} by Gln appears to have selectively decelerated one or more of the reaction steps coming after alcohol oxidation immediately led to the possibility that a relatively stable intermediate could be formed in E161Q under conditions when

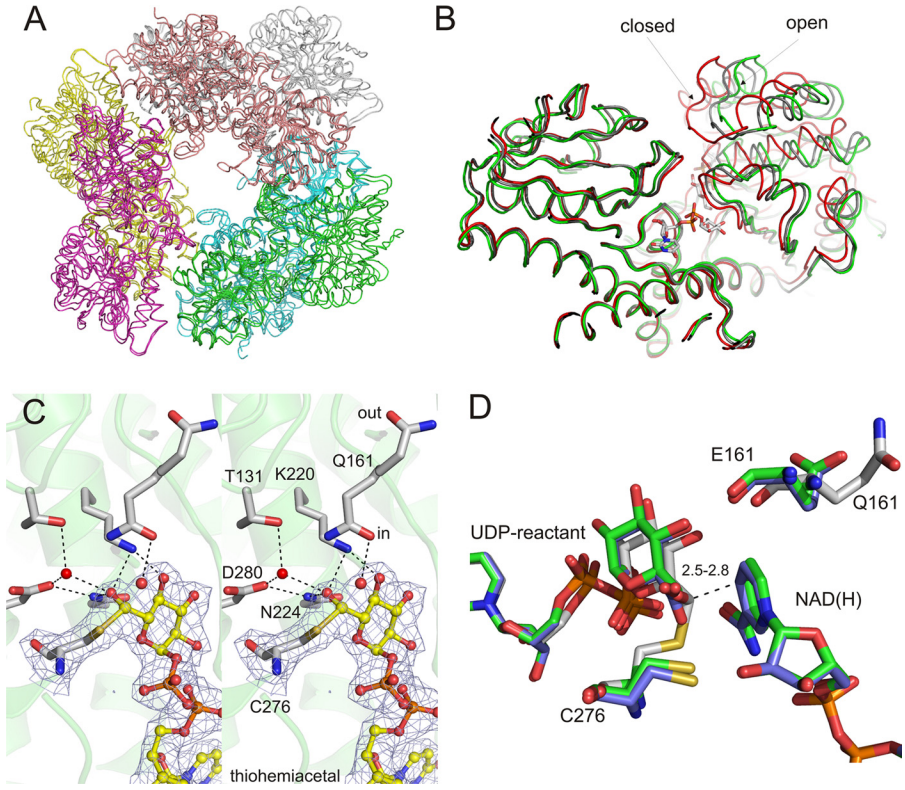

FIGURE 2. **Structural characterization of the E161Q mutant.** *A*, shown is structural superimposition of the homohexamers of E161Q and wild-type hUGDH bound to UDP-Glc and NADH. *B*, shown is superimposition of the protein subunits of E161Q (*gray* schematic, UDP-Glc molecules are shown) and wild-type hUGDH (ternary complex with UDP-Glc and NADH (*red* schematic, closed conformation) and apo structure (*green* schematic, open conformation)). Note that E161Q adopts a quasi-open conformation. *C*, shown is a close-up stereo view of the active site of the thiohemiacetal enzyme intermediate in the E161Q mutant. The electron density map ($2F_o - F_c$, contoured at 1.0 σ) illustrates the presence of the covalent intermediate. Conformation states of Gln^{161} in the in and out positions are shown. Water molecules are shown as *red spheres*, and hydrogen bonding interactions (≤3.1 Å) are depicted by *dashed lines*. *D*, shown is superimposition of the covalently linked substrate in E161Q (*white*, C-atoms) with UDP-Glc (*green*, C-atoms) and UDP-GlcUA (*blue*, C-atoms) bound by wild-type enzyme. The NAD(H) present in the complexes of wild-type enzyme is also shown. The distances between the reactive carbons of substrate (glucosyl C6) and the nicotinamide ring of coenzyme (C4) are shown. The distance is favorable for hydride transfer, suggesting that the thiohemiacetal is bound in a position suitable to become further oxidized by NAD^+.

UDP-Glc is saturating. This was examined by a time-resolved MS experiment.

Upon incubation of E161Q (20 μM) in the presence of saturating concentrations of UDP-Glc (1 mM) and NAD^+ (15 mM), we identified a macromolecular species which accumulated that displayed a +562 ± 0.1 g/mol mass increase relative to apoenzyme. The expected mass increase would be +562 g/mol if a catalytically competent (thio)ester intermediate of E161Q was accumulated in the steady-state phase of substrate conversion (Δmass: +564 g/mol for hemiacetal). Deconvolution of the MS data showed two peaks of similar size, hence presumable abundance: one corresponding to native E161Q and another corresponding to the enzyme intermediate (Fig. 1*C*). The observed $\Pi/[E]$ ratio of 1 for the mutant (Fig. 1*B*) is thus best consistent with an acylenzyme intermediate of E161Q produced in two successive oxidation steps of UDP-Glc. The relative abundance of the covalent intermediate of E161Q was a maximum at steady state (~1 min) and decreased upon prolonged incubation, reflecting the progressing depletion of the limiting UDP-Glc substrate (supplemental Fig. S1). Therefore, this indicates that the presence of unmodified enzyme in the analyzed samples was a true characteristic of the catalytic reaction in solution and did not occur as a result of instability of the covalent intermediate under the conditions of MS analysis.

Crystal Structure of E161Q Mutant Shows Trapped Thiohemiacetal Enzyme Intermediate—E161Q was crystallized in the presence of UDP-Glc and NAD^+, and the structure was determined at 2.3 Å resolution (Table 1; PDB code 3khu). The overall homohexamer structure of the mutant is highly similar to the previously reported structures of hUGDH (Fig. 2*A*). In each subunit of E161Q (Fig. 2*B*), the substrate binding site was occupied by UDP-Glc. Interestingly, the coenzyme binding site in the N-terminal domain did not contain NAD^+, but it had UDP-Glc bound instead. Anchoring of UDP-Glc as the NAD^+ surrogate occurred mainly through its UDP moiety, mimicking the adenine portion of the NAD^+. The corresponding glucosyl moiety appears to have been bound comparatively weakly, exploiting interactions completely different from the ones used for productive binding of the nicotinamide ribose of NAD^+ (see later in text).

Assessment of the electron density in the active sites of all six molecules in the asymmetric unit of the E161Q structure revealed a clear additional, incessant density bridging the UDP-Glc C6 and Cys^{276} Sγ atoms, as shown in Fig. 2*C*. The distance between the carbon and sulfur atoms was <2 Å, where for a

non-bonded interaction the atoms would be expected to have a distance of >3.5 Å (31) (the sum of the van der Waals radii of a carbon and sulfur atom). Therefore, this confirmed the presence of a covalent intermediate on Cys^{276}. Supplemental Fig. S2 provides a stereo depiction of the covalent intermediate. Because the O6 atom of the sugar ring is not coplanar with the C6-Sγ bond, the electron density (Fig. 2*C*) clearly indicates an sp^3-hybridized carbon at the reactive center of the substrate, implying that a tetrahedral thiohemiacetal (not a thioester) intermediate was trapped in the E161Q structure.[3] Limited NAD^+ (2 mM) relative to UDP-Glc (5 mM) plus competition by UDP-Glc for binding to the coenzyme binding site could explain why the E161Q reaction stopped after one round of oxidation in the crystal. Moreover, the low temperature used and high solution viscosity could be additional factors.

Structural comparison of the E161Q intermediate to the wild-type hUGDH bound with UDP-Glc/NADH and UDP-GlcUA/NAD^+ shows that the spatial arrangement of residues in the immediate vicinity of the substrate reactive C6 group was hardly affected by formation of the intermediate (Fig. 2*D*; supplemental Fig. S3). The notable exception is the side chain of Cys^{276}, which has undergone an ~35° rotation in the intermediate structure as compared with the ternary complex structures, displacing the Sγ atom by 2 Å. The position of the glucopyranosyl ring in the substrate binding pocket was unchanged in the intermediate structure as compared with the ternary complex structures. Gln^{161} is seen to adopt two different conformations in and out of the active site, as shown in Fig. 2*C*. A structural overlay of the ternary complexes and the thiohemiacetal intermediate (having Gln^{161} in the out conformation) indicates that the C6 of covalently bound UDP-*gluco*-hexodialdose would be within suitable hydride transfer distance (2.5–2.8 Å) to the nicotinamide C4 (Fig. 2*D*), suggesting that a catalytically competent intermediate has been trapped in the crystal.

Fig. 2*B* displays a structural superimposition of the protein subunits of the E161Q intermediate, the native hUGDH in complex with UDP-Glc/NADH and the apoT131A structure. It was previously shown that upon anchoring of UDP-Glc and NADH to the apoenzyme, the hUGDH subunit undergoes a large "domain closure" conformational change that can be best envisioned as an ~13° rotation of the N-terminal domain toward the assumed immobile C-terminal domain (4). The α10 helix was identified as the hinge region for this rotation. It is very interesting that the E161Q intermediate now adopts a "quasi open" domain orientation that is only 3° different from

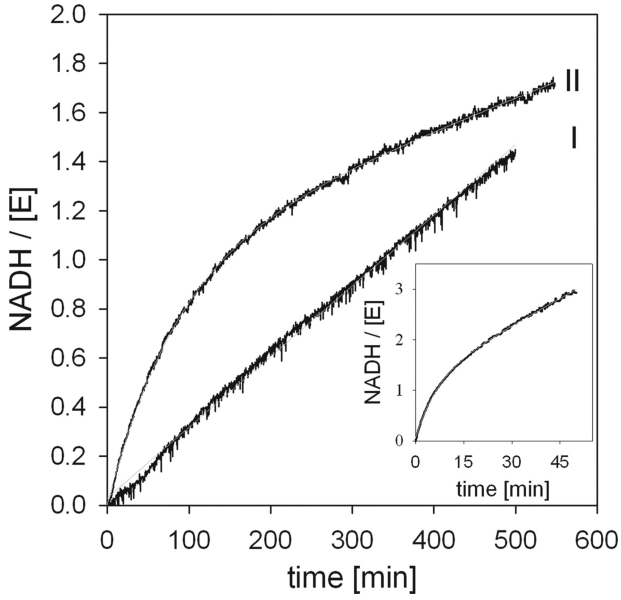

FIGURE 3. **Time course analysis for reactions of D280A (*I*) and K220A (*II*) mutants of hUGDH.** *Inset*, Functional complementation of K220A with methylamine (100 mM) stimulates the reaction rate. The concentrations of UDP-Glc and NAD^+ were 1 and 15 mM, respectively. The molar enzyme concentration was 100 μM. Fits of the appropriate equation to experimental data are shown as *gray lines*.

the "fully open" conformation seen in the apoenzyme (Fig. 2*B*). We interpret this structural feature of E161Q to imply that the mutant has undergone intermittent domain opening to allow for the release of the NADH produced during formation of the thiohemiacetal enzyme intermediate. Attachment of UDP-Glc to the site where NAD^+ normally binds eventually traps the intermediate in the crystal, and unlike binding of NAD^+, UDP-Glc appears to be not sufficient to promote the complete "closing" motion of the N-terminal domain.

Roles of Lys^{220} and Asp^{280} in Covalent Catalysis by hUGDH—The function of Cys^{276} as catalytic nucleophile of the reaction of hUGDH is validated by crystallographic and kinetic evidence on the E161Q mutant (Figs. 1 and 2). However, there is the mechanistically relevant question of participation of the other active-site residues in providing catalytic assistance for covalent intermediate formation. The structure of hUGDH was previously interpreted to support a role of Lys^{220} as the catalytic base for abstraction of alcohol proton in the first oxidation step. An active-site water bonded to Asp^{280} was suggested to deprotonate the thiol side chain of Cys^{276} for nucleophilic attack. However, one caveat of the mechanistic proposal is that supporting biochemical evidence was previously lacking. We, therefore, substituted Lys^{220} and Asp^{280} individually by Ala and performed a kinetic characterization of purified K220A and D280A mutants. Both mutants showed extremely low levels of UGDH activity, consistent with previous findings of Simpson and co-workers (21, 22). Just 75% of a full turnover was observed in ~5 h (Fig. 3), assuming that all active sites present in the assay undergo turnover at the same time and form two NADHs during the reaction. Despite these limitations in terms of steady-state kinetic analysis, the data could be used to derive an estimate for k_{obs}, calculated from observed NADH rate (D280A) or by fitting data with Equation 2

[3] It is interesting to compare the structure of the thiohemiacetal intermediate of E161Q to the structure of a thioacylenzyme intermediate of a E268A mutant of glyceraldehyde 3-phosphate dehydrogenase (GAPN) from *Streptococcus mutans* (32). Just like Glu^{161} in hUGDH, the substituted Glu^{268} of GAPN was the assumed catalytic base for thioester hydrolysis. The crystal structure of the trapped intermediate of the GAPN mutant was solved at a resolution (2.55 Å) similar to that obtained here for the E161Q mutant structure. The flat density shape at C1 of the covalent adduct of GAPN was consistent with the sp^2 hybridization expected for a thioacylenzyme intermediate. We refer to the study of D'Ambrosio *et al.* on GAPN (32) to emphasize that the crystallographic data on the covalent intermediate of E161Q do allow unambiguous distinction between an enzyme-bound hemiacetal and ester.

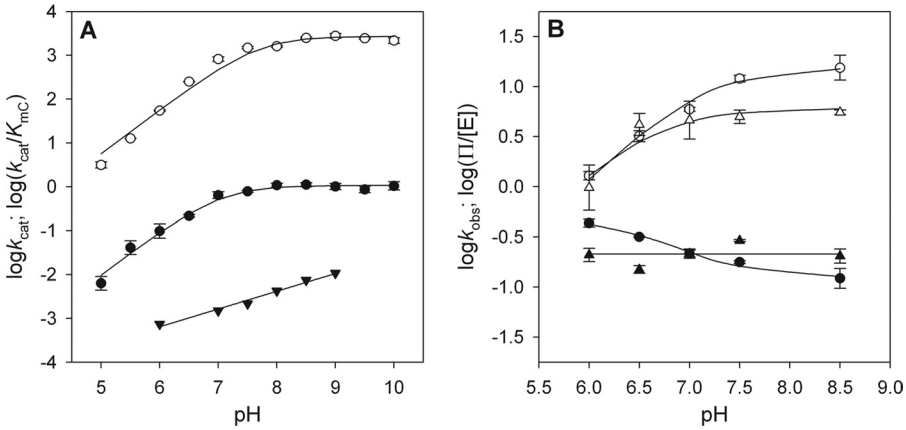

FIGURE 4. **pH profile analysis for wild-type hUGDH and E161Q mutant.** *A*, steady-state kinetic data show k_{cat} for wild-type enzyme (*filled circles*) and E161Q (*down triangles*) and k_{cat}/K_{mC} (*open circles*) for wild-type enzyme. *B*, transient kinetic data were obtained for wild-type hUGDH showing k_{obs} (*open symbols*) and II/[*E*] (*closed symbols*) recorded at high (10 mM; *circles*) and low (0.1 mM; *triangles*) concentration of NAD^+. UDP-Glc was used in a concentration of 1 mM. The *symbols* show the experimental data, and *solid lines* are fits with the suitable equation.

(K220A). The k_{obs} values thus obtained were decreased by about 5 orders of magnitude in comparison to k_{obs} of the wild-type enzyme (supplemental Table S1). The k_{obs} for D280A displayed a linear dependence on the NAD^+ concentration up to 10 mM. The lowered coenzyme binding affinity of D280A compared with wild-type enzyme can probably be explained by disruption of a water-mediated interaction between the side chain of Asp^{280} and the NAD^+ ribose 2-OH, observed in the structure of the enzyme complex with UDP-Glc and NADH (4).

In the Fig. 3 *inset* we show that external methylamine elicited functional complementation of K220A, giving a substantial (k_{obs}, ~20-fold; apparent k_{cat}, ~120-fold) rate enhancement in the conversion of UDP-Glc by the mutant (supplemental Table S1). The "chemical rescue" of K220A displayed a saturable dependence on the methylamine concentration (supplemental Table S1), suggesting that the mutant enzyme is capable of binding the amine, presumably at the site vacated by substitution of Lys^{220} with Ala, and that the enzyme-amine complex is more active than the free K220A enzyme. We also showed that complementation of K220A by methylamine worked best at high pH (supplemental Fig. S4), as expected if the unprotonated form of the amine was required for activity enhancement, which is consistent with participation of the unprotonated ϵ-NH_2 group of Lys^{220} in catalysis. In summary, these results are consistent with the proposed base catalytic function of Lys^{220} during the alcohol oxidation step of the reaction. They also suggest an essential role of the lysine, likely as oxyanion stabilizer, during the second oxidation and thioester hydrolysis.

The kinetic behavior of the D280A mutant (Fig. 3) is interpreted to support that catalysis in the first oxidation step of hUGDH has become massively disrupted as a result of the mutation. This finding fits very well with the idea described in our previous paper on hUGDH that oxidation of UDP-Glc by hydride transfer to NAD^+ is strongly coupled to formation of the thiohemiacetal enzyme intermediate (4). To perform nucleophilic attack on the incipient aldehyde, the side chain of Cys^{276} needs to be activated by deprotonation, and this was thought to occur through just-in-time proton removal by the water molecule coordinated to Asp^{280}. The observed impairment of the D280A mutant can thus probably be explained by loss of participation from covalent catalysis in the alcohol dehydrogenase step of the reaction. In accordance with this notion, both character and magnitude of the disruptive effect on the enzymatic reaction that resulted from complete deletion of the catalytic nucleophile in a C276A mutant of hUGDH (4) were highly similar to the just-described kinetic consequences of the $Asp^{280} \rightarrow$ Ala replacement. Note: the activity of D280A was not rescued by the addition of various anions (chloride, bromide, azide, formate, or acetate).

Besides Lys^{220}, Cys^{276}, and Asp^{280}, there are two other conserved residues in the active site of hUGDH: Thr^{131} and Asn^{224} (Fig. 2*C*). Their importance for UGDH activity was examined in T131S and N224A mutants. Steady-state kinetic parameters of the two mutants were within an order of magnitude of the native enzyme (supplemental Table S1), suggesting that neither residue is essential for catalysis by hUGDH.

Role of Glu^{161} as Catalytic Base for Thioester Hydrolysis, Revealed in pH Studies—So far we have presented evidence that emphasized the importance of Glu^{161} in the catalytic step of thioester hydrolysis. To show the exact role of the Glu in this step, we analyzed the pH dependences of the reaction rate constants for wild-type enzyme and E161Q. Experimental data and their fits with a suitable mathematical model are shown in Fig. 4. Table 3 summarizes the apparent ionization constants determined from the pH profiles. The k_{cat} for wild-type hUGDH was constant at high pH and decreased below a pK of 7.0 (±0.1). The k_{obs} determined at high concentration of NAD^+ displayed essentially the same pH dependence as k_{cat} (pK = 7.1 ± 0.1). The pH dependence of k_{obs} determined at low NAD^+ revealed a substantially lower pK of 6.6 (± 0.3). The observation that k_{obs} of the wild-type enzyme is governed by a different apparent ionization depending on the level of NAD^+ used in the reaction suggests that the rate-limiting step for k_{obs} changes in response to variation of the NAD^+ concentration. This result is consistent with findings from our previous paper on hUGDH, that showed that decreasing the NAD^+ concentration results in a gradual increase in the contribution of the second oxidation

step to the overall rate limitation, which is in k_{cat}. It was specifically proposed that exchange of NADH by NAD^+ progressively becomes the slowest step of the reaction under these conditions, implying that the k_{obs} determined at low NAD^+ includes only steps of the reaction up to the thiohemiacetal intermediate, ready to bind new NAD^+. It was revealing to observe, therefore, that the steady-state rate constant (V_{ss}/E) obtained from stopped-flow progress curves measured at sub-K_{mC} levels of NAD^+ displayed a pH dependence similar to the pH dependence of k_{cat} (pK = 7.6 ± 0.2). The pH-dependent step(s) that controls the pH profile of k_{cat} for the wild-type enzyme must, therefore, be located in the steps used for the second oxidation and hydrolysis.

The k_{cat} for E161Q increased linearly (slope: 0.41 ± 0.03) as the pH was raised from 6.0 to 9.0 (Fig. 4*A*). The apparent ionization of pK = 7.0 present in the pH-log k_{cat} profile of native hUGDH was clearly eliminated from the pH dependence of the mutant. The pH dependence of E161Q conforms with expectation for the consequence of removal of a general base catalytic group from the enzyme and is consistent with a role for specific base catalysis by water/hydroxide ion in the mutant. The proposed function of Glu^{161} implies that protonation of its side chain below its apparent pK should make the catalytic step of thioester hydrolysis progressively more rate-limiting for the k_{cat} of the wild-type enzyme, observable as an increase in the burst magnitude $\Pi/[E]$ upon lowering the pH. One can see in Fig. 4*B* that $\Pi/[E]$ indeed has the predicted pH dependence, increasing from a low constant value at high pH to a higher, also constant value at low pH. The maximum value of $\Pi/[E]$ at high NAD^+ at pH 6.0, where Glu^{161} should be largely protonated, corresponds to about half the molar equivalent of enzyme active sites present in the reaction. Of note, the pH dependence of $\Pi/[E]$ was only seen under conditions of a high concentration of NAD^+. Using a low concentration of NAD^+ to make the second oxidation rate-limiting, $\Pi/[E]$ was independent of pH, as expected because Glu^{161} is not a candidate catalytic residue in this step. In summary, therefore, the evidence from the pH studies strongly supports a role of Glu^{161} as Brønsted catalytic base for hydrolysis of the thioester enzyme intermediate.

TABLE 3
Summary of results of pH studies

log*Y*	wild-type hUGDH p*K*	C	r^2	Equation
Steady state				
k_{cat}	7.0 ± 0.1	1.1 ± 0.1 s^{-1}	0.99	3
k_{cat}/K_{mC}	7.7 ± 0.2	2715 ± 461 $M^{-1}s^{-1}$	0.98	3
Presteady state				
10 mM NAD^+				
k_{obs}	7.1 ± 0.1	15.6 ± 1.5 s^{-1}	0.99	3
V_{ss}	7.3 ± 0.1	1.5 ± 0.1 s^{-1}	0.99	3
$\Pi/[E]$	6.5 ± 0.3	C_H = 0.12 ± 0.01 C_L = 0.5 ± 0.1	0.99	4
100 μM NAD^+				
k_{obs}	6.6 ± 0.3	6 ± 1 s^{-1}	0.88	3
V_{ss}	7.6 ± 0.2	0.4 ± 0.1 s^{-1}	0.99	3
$\Pi/[E]$	No	0.21 ± 0.05[a]		
		E161Q		
k_{cat}	slope: 0.41 ± 0.03		0.98	LR[b]

[a] Average and S.D. of $\Pi/[E]$ obtained in the pH range 6.0–8.5 (see Fig. 4*B*).
[b] LR, linear regression.

The structure of the E161Q thiohemiacetal intermediate provides a very interesting detail about the possible mechanism of thioester hydrolysis, showing that a water molecule bonded to Gln^{161} (3.6 Å) would be in a suitable position to potentially serve as incoming nucleophile for the reaction (Fig. 2*C*). Assuming that a similar arrangement of groups occurs at the level of the thioester intermediate, there is the highly attractive feature that hydrolysis could be achieved through a tetrahedral transition state geometrically analogous to the anionic thiohemiacetal, thus allowing full utilization of the oxyanion-stabilizing capabilities of the hUGDH catalytic center in all three steps of a parsimonious reaction coordinate, summarized in Scheme 2. Although the water coordinated to Asp^{280} has been proposed to be involved in hydrolysis (33), our data indicate that this water is unlikely to participate as reactant in the hydrolysis step. The proposed role of the mobile Glu^{161} in this mechanism involves dis-

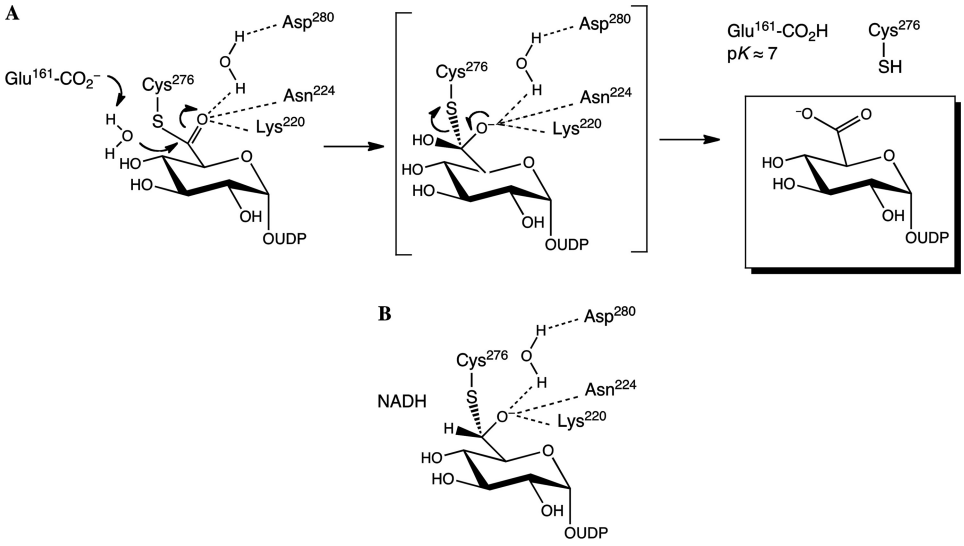

SCHEME 2. *Panel A*, the proposed mechanism of hydrolysis of the thioacylenzyme intermediate of hUGDH shows catalytic assistance from Glu^{161} and stabilization of a tetrahedral oxyanion formed in the course of the reaction. *Panel B*, shown is the proposed analogous stabilization of the anionic thiohemiacetal intermediate formed in the first oxidation step.

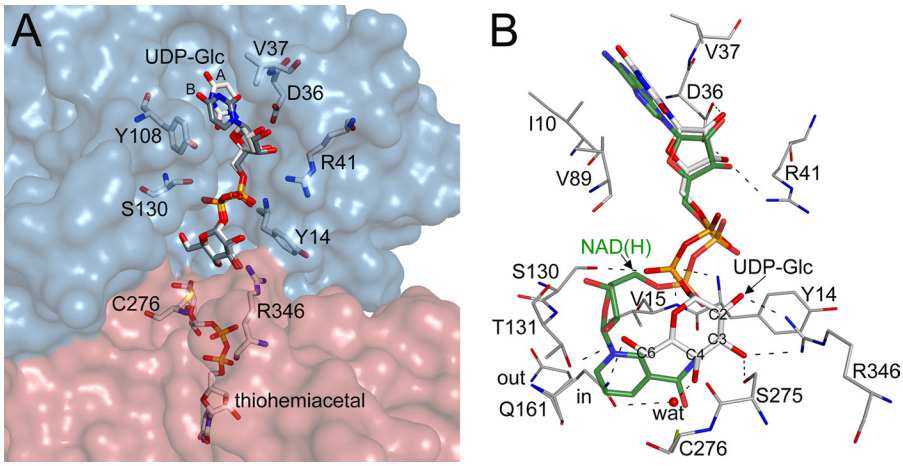

FIGURE 5. **Binding of UDP-Glc at the NAD$^+$ site.** *A*, shown is a surface representation of hUGDH colored with the N-terminal domain (*blue*) and the C-terminal domain (*red*). UDP-Glc ligands from subunits A (*white*, C-atoms) and B (*gray*, C-atoms) are superimposed and shown within the NAD$^+$ binding cleft. *B*, shown is a comparison of UDP-Glc bound to E161Q (*white*, C-atoms) and NADH bound to wild-type hUGDH (*green* C-atoms, from PDB structure 2q3e). Residues within 4 Å of UDP-Glc are shown with hydrogen bonds indicated by *dashed lines*. Glucosyl carbon atoms discussed in the text are labeled and a water molecule that mediates interactions between the C4 hydroxyl, and the in conformation of Gln^{161} is shown as a *red sphere*.

placement of the NADH formed in each oxidation step[4] as well as catalytic deacylation of the enzyme. Of note, a similarly flexible and functional Glu is found in aldehyde dehydrogenases, which resemble UGDH mechanistically in the use of covalent catalysis from a cysteine nucleophile for the oxidation of their aldehyde substrates (32, 34).

Binding of UDP-Glc at NAD$^+$ Binding Site; Practical Effect of an Unexpected Observation?—In the E161Q structure, a second UDP-Glc binds in the cleft on the surface of the N-terminal domain where NAD$^+$ usually binds, with the glucosyl moiety buried within the domain interface. Fig. 5 displays the molecular interactions involved in the accommodation of UDP-Glc at the NAD$^+$ binding site. The UMP moiety of UDP-Glc is mainly bound through its phosphoribosyl part, which forms hydrogen bonds with Asp^{36} and Arg^{41} similarly to the corresponding phosphoribosyl group of NAD$^+$ in the structure of the wild-type enzyme. Depending on the subunit, the uracil is observed in two different conformations, with its O2 atom positioned either toward or away from Tyr^{108} in the hydrophobic pocket that normally accommodates the adenine of NAD$^+$ (Fig. 5*A*). Binding of the glucose 1-phosphate moiety of UDP-Glc involves essentially the same residues responsible for binding of the nicotinamide-ribosyl-phosphate group of NAD$^+$, however, a substantial amount of flexibility of the binding site is observed (supplemental Fig. S5). In particular, Arg^{346} that originally interacted with the phosphate from the NAD$^+$ group now forms bidentate hydrogen bonds with the hydroxyls at glucosyl C2 and C3 (Fig. 5*B*). Interestingly, a highly similar interaction from Arg^{260} is utilized for accommodating the glucosyl moiety of UDP-Glc at the substrate binding site. The UDP-Glc phosphates interact with the main-chain nitrogens of Tyr^{14} and Val^{15}, which are embedded within the ^{11}G*X*G*XX*G^{16} repeat at the N terminus of helix α1 that normally binds the NAD$^+$ phosphates, but also make an additional interaction with the side chain of Ser^{130}. Fig. 5*B* further shows that the hydroxyls at glucosyl C3 and C6 of the UDP-Glc inhibitor are likewise involved in hydrogen bonding interactions, and these were previously not utilized for binding of NAD$^+$.

The glucosyl moiety of bound UDP-Glc is shifted ~5 Å compared with the nicotinamide ring in the wild-type enzyme structure, which places the glucose near the Tyr^{14} side chain (supplemental Fig. S5). This shift allows Gln^{161} to be in the "in" conformation without sterically interfering with binding of the inhibitor UDP-Glc molecule. A water-mediated contact between Gln^{161} and the sugar C4 hydroxyl could contribute to stabilization of the glutamine in the in conformation. These results reveal the ability of the NAD$^+$ binding site of E161Q to exploit induced fit in the creation of an apparently fully developed binding pocket for the glucosyl moiety of a UDP-Glc inhibitor. It could be interesting to further explore the promiscuity of the binding site for the purpose of targeted enzyme inhibition.

In conclusion, participation of covalent catalysis in the reaction mechanism of hUGDH has been elucidated comprehensively. The mechanistic proposal derived from the evidence presented involves for the first time a clear assignment of catalytic function to each individual group in the active site of the enzyme. The UDP-Glc molecule attached to the coenzyme binding site of thiohemiacetal enzyme intermediate of E161Q provides the first case of NAD$^+$ antagonism in hUGDH and could, therefore, assist in the development of inhibitors of the enzyme.

Acknowledgments—We thank Dr. Kunde Guo (Structural Genomics Consortium) for cloning of hUGDH mutants. Dr. Panagis Filippakopoulos, Dr. Ivan Alfano, and Prof. Stefan Knapp (all with the Structural Genomics Consortium) are gratefully acknowledged for assistance, helpful discussions, and suggestions. We thank Dr. Frank von Delft (Structural Genomics Consortium) for data collection at the Diamond Light Source.

[4] The observed decrease in k_{cat}/K_{mC} resulting from replacement of Glu^{161} by Gln is thus explained. The role of Glu^{161} during binding of UDP-Glc to free hUGDH (k_{cat}/K_{mS}) is not known. Considering the crystallographic data from this and a previous study of hUGDH (4), we believe that this role is probably indirect.

REFERENCES

1. Egger, S., Chaikuad, A., Kavanagh, K. L., Oppermann, U., and Nidetzky, B. (2010) UDP-glucose dehydrogenase. Structure and function of a potential drug target. *Biochem. Soc. Trans.* **38,** 1378–1385
2. Tukey, R. H., and Strassburg, C. P. (2000) Human UDP-glucuronosyltransferases. Metabolism, expression, and disease. *Annu. Rev. Pharmacol. Toxicol.* **40,** 581–616
3. Campbell, R. E., Mosimann, S. C., van De Rijn, I., Tanner, M. E., and Strynadka, N. C. (2000) The first structure of UDP-glucose dehydrogenase reveals the catalytic residues necessary for the 2-fold oxidation. *Biochemistry* **39,** 7012–7023
4. Egger, S., Chaikuad, A., Kavanagh, K. L., Oppermann, U., and Nidetzky, B. (2011) Structure and mechanism of human UDP-glucose 6-dehydrogenase. *J. Biol. Chem.* **286,** 23877–23887
5. Kadirvelraj, R., Sennett, N. C., Polizzi, S. J., Weitzel, S., and Wood, Z. A. (2011) Role of packing defects in the evolution of allostery and induced fit in human UDP-glucose dehydrogenase. *Biochemistry* **50,** 5780–5789
6. Chen, Y. Y., Ko, T. P., Lin, C. H., Chen, W. H., and Wang, A. H. (2011) Conformational change upon product binding to *Klebsiella pneumoniae* UDP-glucose dehydrogenase. A possible inhibition mechanism for the key enzyme in polymyxin resistance. *J. Struct. Biol.* **175,** 300–310
7. Rocha, J., Popescu, A. O., Borges, P., Mil-Homens, D., Moreira, L. M., Sá-Correia, I., Fialho, A. M., and Frazão, C. (2011) Structure of *Burkholderia cepacia* UDP-glucose dehydrogenase (UGD) BceC and role of Tyr^{10} in final hydrolysis of UGD thioester intermediate. *J. Bacteriol.* **193,** 3978–3987
8. Nelsestuen, G. L., and Kirkwood, S. (1971) *J. Biol. Chem.* **246,** 3824–3834
9. Ordman, A. B., and Kirkwood, S. (1977) UDP-glucose dehydrogenase. Kinetics and their mechanistic implications. *Biochim. Biophys. Acta* **481,** 25–32
10. Ordman, A. B., and Kirkwood, S. (1977) Mechanism of action of uridine diphoglucose dehydrogenase. Evidence for an essential lysine residue at the active site. *J. Biol. Chem.* **252,** 1320–1326
11. Ridley, W. P., Houchins, J. P., and Kirkwood (1975) Mechanism of action of uridine diphosphoglucose dehydrogenase. Evidence for a second reversible dehydrogenation step involving an essential thiol group. *J. Biol. Chem.* **250,** 8761–8767
12. Ridley, W. P., and Kirkwood (1973) The stereospecificity of hydrogen abstraction by uridine diphosphoglucose dehydrogenase. *Biochem. Biophys. Res. Commun.* **54,** 955–960
13. Schiller, J. G., Bowser, A. M., and Feingold, D. S. (1972) Studies on the mechanism of action of UDP-D-glucose dehydrogenase from beef liver. *Carbohydr. Res.* **21,** 249–253
14. Franzen, J. S., Kuo, I., Eichler, A. J., and Feingold, D. S. (1973) UDP-glucose dehydrogenase. Substrate binding stoichiometry and affinity. *Biochem. Biophys. Res. Commun.* **50,** 517–523
15. Franzen, J. S., Ishman, R., and Feingold, D. S. (1976) Half-of-the-sites reactivity of bovine liver uridine diphosphoglucose dehydrogenase toward iodoacetate and iodoacetamide. *Biochemistry* **15,** 5665–5671
16. Eccleston, E.D., Thayer, M.L., and Kirkwood, S. (1979) Mechanisms of action of histidinol dehydrogenase and UDP-Glc dehydrogenase. Evidence that the half-reactions proceed on separate subunits. *J. Biol. Chem.* **254,** 11399–11404
17. Ge, X., Campbell, R. E., van de Rijn, I., and Tanner, M. E. (1998) Covalent adduct formation with a mutated enzyme: evidence for a thioester intermediate in the reaction catalyzed by UDP-glucose dehydrogenase. *J. Am. Chem. Soc.* **120,** 6613–6614
18. Campbell, R. E., Sala, R. F., van de Rijn, I., and Tanner, M. E. (1997) Properties and kinetic analysis of UDP-glucose dehydrogenase from group A streptococci. Irreversible inhibition by UDP-chloroacetol. *J. Biol. Chem.* **272,** 3416–3422
19. Ge, X., Penney, L. C., van de Rijn, I., and Tanner, M. E. (2004) Active site residues and mechanism of UDP-glucose dehydrogenase. *Eur. J. Biochem.* **271,** 14–22
20. Campbell, R. E., and Tanner, M. E. (1999) UDP-Glucose analogues as inhibitors and mechanistic probes of UDP-glucose dehydrogenase. *J. Org. Chem.* **64,** 9487–9492
21. Easley, K. E., Sommer, B. J., Boanca, G., Barycki, J. J., and Simpson, M. A. (2007) Characterization of human UDP-glucose dehydrogenase reveals critical catalytic roles for lysine 220 and aspartate 280. *Biochemistry* **46,** 369–378
22. Sommer, B. J., Barycki, J. J., and Simpson, M. A. (2004) Characterization of human UDP-glucose dehydrogenase. Cys-276 is required for the second of two successive oxidations. *J. Biol. Chem.* **279,** 23590–23596
23. Clarkin, C. E., Allen, S., Kuiper, N. J., Wheeler, B. T., Wheeler-Jones, C. P., and Pitsillides, A. A. (2011) Regulation of UDP-glucose dehydrogenase is sufficient to modulate hyaluronan production and release, control sulfated GAG synthesis, and promote chondrogenesis. *J. Cell. Physiol.* **226,** 749–761
24. Clarkin, C. E., Allen, S., Wheeler-Jones, C. P., Bastow, E. R., and Pitsillides, A. A. (2011) Reduced chondrogenic matrix accumulation by 4-methylumbelliferone reveals the potential for selective targeting of UDP-glucose dehydrogenase. *Matrix Biol.* **30,** 163–168
25. Collaborative Computational Project, Number 4 (1994) The CCP4 suite. Programs for protein crystallography. *Acta Crystallogr. D* **50,** 760–763
26. Leslie, A. G. (1999) Integration of macromolecular diffraction data. *Acta Crystallogr. D* **55,** 1696–1702
27. McCoy, A. J. (2007) Solving structures of protein complexes by molecular replacement with Phaser. *Acta Crystallogr. D* **63,** 32–41
28. Emsley, P., and Cowtan, K. (2004) Coot, Model-building tools for molecular graphics. *Acta Crystallogr. D* **60,** 2126–2132
29. Murshudov, G. N., Vagin, A. A., and Dodson, E. J. (1997) Refinement of macromolecular structures by the maximum-likelihood method. *Acta Crystallogr. D* **53,** 240–255
30. Gasteiger, E., Hoogland, C., Gattiker, A., Duvaud, S., Wilkins, M. R., Appel, R. D., and Bairoch, A. (2005) in *The Proteomics Protocols Handbook* (John M. Walker, ed) pp. 571–607, Humana Press, Totowa, NJ
31. Tsai, J., Taylor, R., Chothia, C., and Gerstein, M. (1999) The packing density in proteins. Standard radii and volumes. *J. Mol. Biol.* **290,** 253–266
32. D'Ambrosio, K., Pailot, A., Talfournier, F., Didierjean, C., Benedetti, E., Aubry, A., Branlant, G., and Corbier, C. (2006) The first crystal structure of a thioacylenzyme intermediate in the ALDH family. New coenzyme conformation and relevance to catalysis. *Biochemistry* **45,** 2978–2986
33. Rajakannan, V., Lee, H. S., Chong, S. H., Ryu, H. B., Bae, J. Y., Whang, E. Y., Huh, J. W., Cho, S. W., Kang, L. W., Choe, H., and Robinson, R. C. (2011) Structural basis of cooperativity in human UDP-glucose dehydrogenase. *PLoS ONE* **6,** e25226
34. Muñoz-Clares, R. A., González-Segura, L., and Díaz-Sánchez, A. G. (2011) Crystallographic evidence for active-site dynamics in the hydrolytic aldehyde dehydrogenases. Implications for the deacylation step of the catalyzed reaction. *Chem.-Biol. Interact.* **191,** 137–146